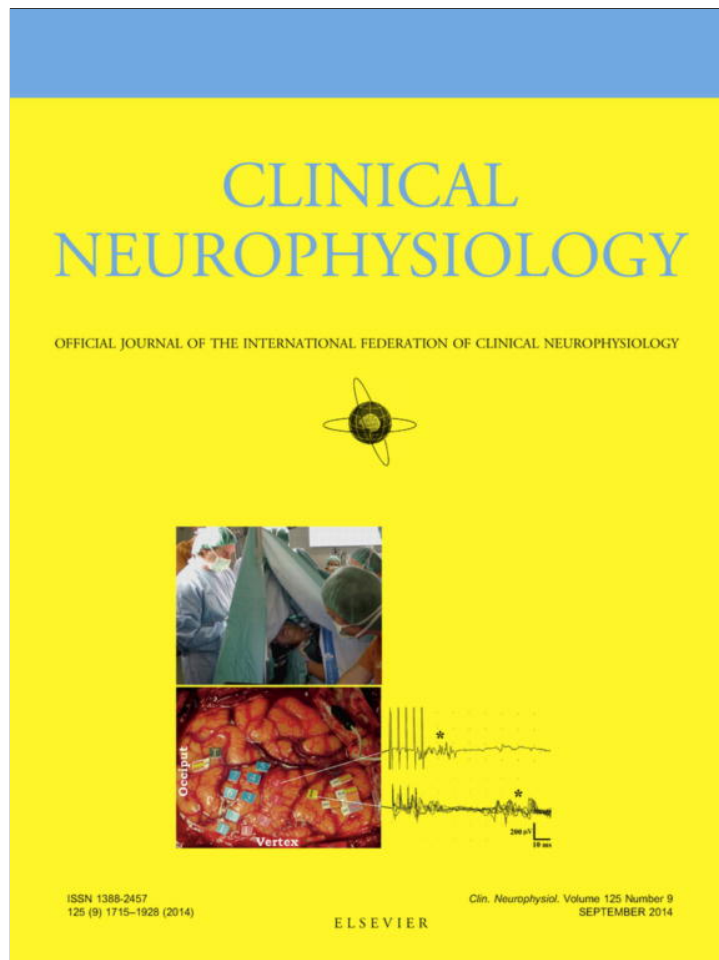


Provided for non-commercial research and education use.
Not for reproduction, distribution or commercial use.

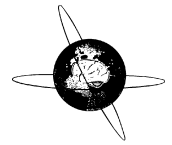


This article appeared in a journal published by Elsevier. The attached copy is furnished to the author for internal non-commercial research and education use, including for instruction at the authors institution and sharing with colleagues.

Other uses, including reproduction and distribution, or selling or licensing copies, or posting to personal, institutional or third party websites are prohibited.

In most cases authors are permitted to post their version of the article (e.g. in Word or Tex form) to their personal website or institutional repository. Authors requiring further information regarding Elsevier's archiving and manuscript policies are encouraged to visit:

<http://www.elsevier.com/authorsrights>



Graph theoretical analysis reveals disrupted topological properties of whole brain functional networks in temporal lobe epilepsy



Junjing Wang^{a,1}, Shijun Qiu^{b,1}, Yong Xu^a, Zhenyin Liu^b, Xue Wen^a, Xiangshu Hu^c, Ruibin Zhang^a, Meng Li^a, Wensheng Wang^{d,*}, Ruiwang Huang^{a,*}

^a Center for the Study of Applied Psychology, Key Laboratory of Mental Health and Cognitive Science of Guangdong Province, School of Psychology, South China Normal University, Guangzhou 510631, China

^b Department of Medical Image Center, Nanfang Hospital, Southern Medical University, Guangzhou 510515, China

^c Department of Epilepsy Diagnosis and Treatment Center, Guangdong 999 Brain Hospital, Guangzhou 510510, China

^d Department of Medical Image Center, Guangdong 999 Brain Hospital, Guangzhou 510510, China

See Editorial, pages 1715–1716

ARTICLE INFO

Article history:

Accepted 12 December 2013

Available online 26 February 2014

Keywords:

Functional networks

Graph theory

Efficiency

Duration of epilepsy

HIGHLIGHTS

- Graph theory and resting fMRI were used to compare brain networks in temporal lobe epilepsy patients and controls.
- Epilepsy patients showed greater clustering between nodes and longer path length than controls.
- Memory and language nodes were abnormally connected with other nodes in epilepsy.

ABSTRACT

Objective: Temporal lobe epilepsy (TLE) is one of the most common forms of drug-resistant epilepsy. Previous studies have indicated that the TLE-related impairments existed in extensive local functional networks. However, little is known about the alterations in the topological properties of whole brain functional networks.

Method: In this study, we acquired resting-state BOLD-fMRI (rsfMRI) data from 26 TLE patients and 25 healthy controls, constructed their whole brain functional networks, compared the differences in topological parameters between the TLE patients and the controls, and analyzed the correlation between the altered topological properties and the epilepsy duration.

Results: The TLE patients showed significant increases in clustering coefficient and characteristic path length, but significant decrease in global efficiency compared to the controls. We also found altered nodal parameters in several regions in the TLE patients, such as the bilateral angular gyri, left middle temporal gyrus, right hippocampus, triangular part of left inferior frontal gyrus, left inferior parietal but supramarginal and angular gyri, and left parahippocampus gyrus. Further correlation analysis showed that the local efficiency of the TLE patients correlated positively with the epilepsy duration.

Conclusion: Our results indicated the disrupted topological properties of whole brain functional networks in TLE patients.

Significance: Our findings indicated the TLE-related impairments in the whole brain functional networks, which may help us to understand the clinical symptoms of TLE patients and offer a clue for the diagnosis and treatment of the TLE patients.

© 2014 International Federation of Clinical Neurophysiology. Published by Elsevier Ireland Ltd. All rights reserved.

* Corresponding authors. Address: Center for Studies of Psychological Application, Key Laboratory of Mental Health and Cognitive Science of Guangdong Province, School of Psychology, South China Normal University, Guangzhou 510631, China. Tel./fax: +86 20 8521 6499 (R. Huang). Tel./fax: +86 20 8763 3769 (W. Wang).

E-mail addresses: wangwensheng36@163.com (W. Wang), ruiwang.huang@gmail.com (R. Huang).

¹ These authors contributed equally to this work.

1. Introduction

Temporal lobe epilepsy (TLE) is one of the most common forms of drug-resistant epilepsy, in which seizures originate from the temporal lobe and propagate through interconnected brain networks limited to or extending beyond the temporal lobe (Guye et al., 2006). In TLE patients, the normal pattern of brain activity is generally believed to become disturbed, causing strange sensations, emotions, and behaviors (Gupta et al., 2007). With the development of neuroimaging techniques, an increasing number of studies have begun to evaluate the impact of TLE on brain networks (Bernhardt et al., 2012; Bettus et al., 2009; Bonilha et al., 2004; Sidhu et al., 2013).

Resting-state functional magnetic resonance imaging (rsfMRI) has been widely used to explore the intrinsic functional organization of the human brain (Anand et al., 2009; Greicius, 2008; Lynall et al., 2010). Based on rsfMRI data, several studies have revealed the TLE-related alterations in some specific local functional networks, such as the epileptogenic network (Bettus et al., 2009; Morgan et al., 2010), default mode network (DMN) (Liao et al., 2011; Zhang et al., 2010), and functional networks of language (Brazdil et al., 2005), memory (Voets et al., 2009), attention (Zhang et al., 2009b), alertness (Zheng et al., 2012), and perception (Zhang et al., 2009a). For example, Bettus et al. (2009) studied the basal functional connectivity (FC) within the temporal lobe in 11 TLE patients and 26 controls, and detected the decreased basal FC within epileptogenic networks. Zhang et al. (2009b) extracted the dorsal attention network using the independent component analysis (ICA), compared the FC in this network between 24 TLE patients and 24 controls, and found decreased FC in almost all the regions of dorsal attention networks in TLE patients. Actually, the whole brain can be modeled as a large-scale complex network, and its function can be fulfilled through simultaneously segregated or integrated specific FC patterns (He and Evans, 2010; van den Heuvel and Hulshoff Pol, 2010) with optimized efficiency (Bassett and Bullmore, 2006). The investigation of TLE-related alterations in the whole brain functional networks, instead of the FC in specific local networks, may give further network-level information about the pathology of TLE patients.

Graph theory offers a framework to quantify topological properties of a complex network, including the global and nodal properties. The whole brain functional network analysis has been widely used to study human brain development (Bullmore and Sporns, 2009) and to detect alterations of brain function in neuropsychiatry-related brain disorders, such as schizophrenia (Liu et al., 2008), attention-deficit/hyperactivity disorder (Wang et al., 2009b), and Alzheimer's disease (Supekar et al., 2008). For the TLE patients, Liao et al. (2010) studied the brain functional networks alterations using the rsfMRI data, but they mainly focused on the altered inter-regional FC in TLE patients. Up to now, little is known about the TLE-related alterations in topological properties, especially the topological efficiency, of the whole brain functional networks during resting state. Very few studies reported the relationship between the altered topological properties and an influential factor of epilepsy duration (Akman et al., 2010; Bernhardt et al., 2009; Bartolomei et al., 2013; Edefonti et al., 2011; van Dellen et al., 2009).

With the aim to investigate the TLE-related alterations in network properties, we constructed whole brain functional networks with rsfMRI data for the TLE patients and the controls, and compared their topological properties of the whole brain functional networks using graph theory analysis. In addition, we assessed the relationship between altered topological properties and the duration of epilepsy.

2. Materials and methods

2.1. Participants

Twenty-six TLE patients were recruited from the Guangdong 999 Brain Hospital. All patients underwent a comprehensive clinical evaluation including a careful interview, neurological examination, neuropsychological assessment, and neurophysiological monitoring according to the epilepsy classification of the International League Against Epilepsy ILAE (1989). Specifically, all patients had: (1) symptoms of TLE (such as complex partial seizures) and typical symptoms of TLE (such as abnormal emotional experiences and psychiatric symptoms, including depression, anxiety, confusion, and cognitive dysfunctions with memory and language complaints); (2) standard electroencephalogram (EEG) and video-EEG evaluations that clearly indicated interictal discharges in the unilateral temporal lobe; and (3) MRI manifestation of unilateral hippocampal sclerosis. In order to avoid confounding factors, we also excluded the patients with: (1) a history of neurological or psychiatric disorders other than TLE in this study; (2) mass lesion (tumor, vascular malformation, or malformations of cortical development) or traumatic brain injury; and (3) mismatch between the EEG localization and the clinical evidence. At last, a combination of EEGs and MRI was used to lateralize the focal side. Thus, all patients in this study were divided into two types: left TLE (lTLE) (three females and 10 males, 22.00 ± 5.07 years) and right TLE (rTLE) (five females and eight males, 26.31 ± 10.10 years). At the time of study, patients were on AED treatment with carbamazepine (200 mg/time, twice/day). All patients had discontinued antiepilepsy medication for about 24 h prior to the scans, and no seizure occurred during this period. The halt of medication might avoid or reduce its effects on the brain functions.

We also recruited 25 age- and gender-matched healthy volunteers (eight females and 17 males, 24.24 ± 5.31 years) as the controls from the staff of the Guangzhou 999 Brain Hospital by advertisement. All of the controls were interviewed to confirm that they had no history of neurological or psychiatric disorders or head injuries. Table 1 lists the demographic information of the TLE patients and the controls. All participants were right handed according to their self-report, and written informed consent was obtained from each participant prior to the study. The protocols were approved by the Institutional Review Board of the Guangdong 999 Brain Hospital, Guangzhou, China.

2.2. Data acquisition

MRI data were acquired on a 1.5 T Philips Intera MR scanner with an eight-channel phased array head coil. The rsfMRI data were obtained along the AC-PC plane using a GE-EPI sequence with the following parameters: repetition time (TR) = 3000 ms, echo time (TE) = 50 ms, flip angle (FA) = 90°, field of view (FOV) = 230 × 230 mm, data matrix = 128 × 128, slice thickness = 4.5 mm, gap = 0 mm, 31 interleaved slices covering the brain, and 160 volumes acquired in 8 min. During the scanning, all the participants were instructed to keep their eyes closed and not to think about anything in particular. In addition, we also acquired 3D high-resolution structural images for each subject with a T1-weighted MP-RAGE (magnetization-prepared rapid gradient echo) sequence. The sequence parameters were TR/TE/FA = 25 ms/4.6 ms/30°, data matrix = 256 × 256, FOV = 240 × 240 mm, slice thickness = 1.2 mm, and 140 sagittal slices. For each participant, both the rsfMRI data and the structural images were obtained in the same session.

Table 1
Demographic and clinical characteristics of participants in this study.

Characteristics	ITLE (n = 13)	rTLE (n = 13)	NC (n = 25)	p-Value (ITLE vs. NC)	p-Value (rTLE vs. NC)
Age (years)	22.00 ± 5.07 (22)	26.31 ± 10.10 (25)	24.24 ± 5.31 (24)	0.376 ^a	0.74 ^a
Gender (F/M)	3/10	5/8	8/17	0.714 ^b	0.73 ^b
Duration (years)	9.97 ± 7.42 (9)	10.62 ± 9.07 (10)	n.a	n.a	n.a

Note: Age of participants and duration of the epilepsy are shown with mean ± SD (median). Abbreviations: ITLE (rTLE), left (right) temporal lobe epilepsy; NC, normal controls; SD, standard deviation, n.a., not applicable.

^a The p-value was obtained using a two-sample two-tailed t-test.

^b The p-value was obtained using a two-tailed Pearson's χ^2 -test.

2.3. Data preprocessing

The fMRI datasets were preprocessed using SPM8 (<http://www.fil.ion.ucl.ac.uk/spm>) and DPARSF (Yan and Zang, 2010). For each participant, the first 10 images were discarded to ensure the magnetization equilibrium. The remaining 150 images were then corrected for the acquisition time delay between different slices and then realigned to the first volume for head-motion correction. We obtained the time course for the head motions by estimating the translations in each direction and the rotations on each axis and ensured that all the participants met the criteria of head motion < 2 mm of displacement or 2° of rotation in any direction. The images were spatially normalized to the Montreal Neurological Institute (MNI) standard space and resampled at a $3 \times 3 \times 3$ mm³ resolution. No spatial smoothing was applied by following previous studies (Achard and Bullmore, 2007; Braun et al., 2012; Wang et al., 2009a). Finally, the waveform for each voxel was passed through a band-pass filter (0.01–0.08 Hz) to reduce the effects of low-frequency drift and high-frequency physiological noise (Liu et al., 2008).

2.4. Construction of brain functional networks

The human brain correlation matrix was constructed according to the automated anatomical labeling (AAL) atlas (Tzourio-Mazoyer et al., 2002), which parcellates the brain into 90 cortical and subcortical regions. The names and abbreviations of these regions of interest (ROIs) are listed in Supplementary Table S1. For each ROI, the mean time series was obtained by averaging the fMRI time courses over all the voxels. Then, we regressed out the influence of head motion, global mean signal, and white matter as well as cerebrospinal fluid (CSF) on the datasets by using multiple linear regression analysis (Fox et al., 2005, 2009; Liu et al., 2008). The residual of this regression was used to substitute for the raw mean time series of the corresponding ROI. Finally, we calculated Pearson's correlation coefficient between the residual time series of each pair of the 90 regions, and determined a 90×90 correlation matrix for each participant. In order to construct the brain functional network for each participant, we took each ROI as a node and the value of the interregional correlation coefficient as the weight of the edge. Thus, we obtained a weighted symmetric FC matrix for each participant. The topological properties of the network were subsequently estimated, based on a weighted FC matrix, according to graph theory (see Supplementary Fig. S1).

2.5. Network analysis

2.5.1. Global parameters

We used six global parameters, the clustering coefficient (C_w), characteristic path length (L_w), normalized weighted clustering coefficient (γ), normalized weighted characteristic path length (λ), global efficiency (E_{glob}), and local efficiency (E_{loc}), to characterize the global properties of the brain functional networks. Their definitions and descriptions are listed in Supplementary Table S2 and are given in a reference (Rubinov and Sporns, 2010).

The small-world properties of a network were characterized by the normalized clustering coefficient, $\gamma = C_w^{real}/C_w^{rand}$, and the normalized characteristic path length, $\lambda = L_w^{real}/L_w^{rand}$ (Watts and Strogatz, 1998), where C_w^{rand} and L_w^{rand} are the averaged weighted clustering coefficient and characteristic path length of 100 matched random networks that keep the same number of nodes, edges, and degree distributions as the real networks. Typically, a small-world network should meet the following criteria: $\gamma \gg 1$ and $\lambda \approx 1$ (Watts and Strogatz, 1998), or $\sigma = \gamma/\lambda > 1$ (Humphries et al., 2006).

2.5.2. Nodal parameters

Three parameters, nodal strength (S_i^w), nodal efficiency (E_i^w), and nodal betweenness (B_i^w), were adopted to describe the nodal properties of the brain functional networks. Their definitions and descriptions are also listed in Supplementary Table S2.

In fact, all the elements of the connectivity matrix can be thresholded by using a preselected measure of sparsity (the ratio between the total number of edges and the maximum possible number of edges in a network), and the choice of a sparsity value has a major effect on the topological organization of networks (Rubinov and Sporns, 2010; Tian et al., 2011). By setting a specific sparsity as the threshold, we are able to assure the same number of network edges for each participant. In order to balance the prominence of the small-world attribute with an appropriate level of sparseness in the networks for all subjects, we determined the range of sparsity according to the following criteria: (1) the average degree $> \log(N)$ (Fornito et al., 2010; Watts and Strogatz, 1998), the average degree being equal to the total number of edges divided by $N/2$ ($N = 90$ in this study) over all nodes of each network, and (2) $\gamma > 1.1$ for all subjects (Tian et al., 2011; Watts and Strogatz, 1998). By this procedure, the range of sparsity ($0.10 \leq \text{sparsity} \leq 0.24$) at the interval of 0.01 was generated. Therefore, the analysis of the network parameters was based on a series of weighted 90×90 FC matrices over the range of $0.10 \leq \text{sparsity} \leq 0.24$ for each participant.

Instead of selecting parameters corresponding to a single sparsity threshold, we used the integrated network parameters over the range of sparsity to detect the between-group differences in the topological parameters of the brain functional networks (Tian et al., 2011). The integrated network parameters were used for further analysis.

The integrated global parameters were defined as

$$X_{glob}^{int} = \sum_{k=10}^{24} X(k\Delta s)\Delta s, \quad (1)$$

where Δs is the sparsity interval of 0.01, and $X(k\Delta s)$ is one of the global network parameters (C_w , L_w , γ , λ , E_{loc} , and E_{glob}) at a sparsity of $k\Delta s$. Similarly, the integrated nodal parameters can be defined as (Tian et al., 2011):

$$Y_{nod}^{int} = \sum_{k=10}^{24} Y(i, k\Delta s)\Delta s, \quad (2)$$

where $Y(i, k, \Delta s)$ represents any of the nodal parameters (S_i^w , E_i^w , and B_i^w) at a sparsity of $k\Delta s$, and where Δs is the sparsity interval of 0.01.

2.5.3. Hub regions

Hubs are highly connected nodes in a network. The nodes with high weighted strength can be regarded as hub regions, which are most likely to have a vital role in the brain functional network. In order to determine the hubs in the functional networks, we calculated the normalized nodal parameters for each node as follows:

$$Y_{nod}^{norm} = \frac{\sum_{k=1}^M Y_{nod}^{int}(i, k)}{\frac{1}{N} \sum_{j=1}^N \sum_{k=1}^M Y_{nod}^{int}(i, k)} \quad (3)$$

where $Y_{nod}^{int}(i, k)$ represents any of the nodal parameters (S_i^{int} , E_i^{int} , and B_i^{int}) at node i for the network of participant k , M is the number of participants, and N is the number of nodes. We identified node i as the hub if the normalized nodal betweenness satisfies the following criterion,

$$B_i^{norm} > mean(\cdot) + SD(\cdot), \quad (4)$$

where $mean(\cdot)$ and $SD(\cdot)$ stand for the averaged value and standard deviation of B_i^{norm} across all nodes of the network, respectively. According to the above description, we determined the hubs of the human brain functional networks corresponding to the ITLE patients, the rTLE patients, and the controls.

2.5.4. Network robustness analysis

Network robustness, characterized by the degree of tolerance against random failures and targeted attack, is usually associated with the stability of a complex network. In the “random failure analysis”, we successively randomly removed nodes from the networks in each subject group. In the “targeted attack analysis”, we removed the nodes in the decreasing order of the value of B_i^{int} . This method captures the influence of a node on the information flow in the network, because network information flow tends to follow the shortest paths. Each time, after removing a node from the network, we recalculated the size of the largest connected component (Bernhardt et al., 2011; He et al., 2008). More robust networks retain a larger connected component even when several nodes have been knocked out.

2.6. Reproducibility analysis

In order to check the reproducibility of our results, we adopted the following two procedures to repeat the network analysis for both the TLE patients and the controls.

2.6.1. Preprocessing schemes

Previous studies (Braun et al., 2012; Wang et al., 2011) have revealed that different preprocessing schemes, such as whether regressing out the global signal or not, may affect the results of network analysis. To confirm the findings of our network analysis based on the main scheme (the non-smoothing rsfMRI data were used to construct the whole brain FC matrix, the interregional correlation was taken as the matrix element, and the node was determined according to the AAL-90 atlas), we also adopted two other schemes, termed as Smoothing scheme and Positive-network scheme, to repeat our network analysis. In the Smoothing scheme, we used the spatial-smoothed rsfMRI data (FWHM = 6 mm) to construct brain networks, while in the Positive-network scheme, we constructed the network based on the positive-only interregional correlations, i.e., we excluded negative correlations. The calculation steps in these two schemes were same as the main scheme except for the respective changes.

2.6.2. Parcellation schemes

The choice of parcellation scheme can affect the topological parameters of network (de Reus and van den Heuvel, 2013; Wang et al., 2009a). In order to confirm the findings derived from the main scheme, we also repeated the calculation by defining the network nodes according to the Harvard-Oxford atlas (HOA-112 atlas) (Kennedy et al., 1998) and the Dos-160 atlas (Dosenbach atlas consisting of 160 ROIs derived from meta-analysis) (Dosenbach et al., 2010). In addition, the calculation steps in these two schemes were exactly similar to the main scheme except for the respective changes.

2.7. Statistical analysis

A nonparametric permutation test (Bullmore et al., 1999) was used to identify significant differences in the topological parameters of brain functional networks between either of the ITLE or rTLE patients and the controls. To find the between-group differences in the global parameters, nodal parameters, and the largest component size, we performed 10,000 permutations and selected $p = 0.05$ (Bonferroni correction) as the threshold to determine significant between-group difference.

Once significant between-group differences were observed in a given nodal parameter, we estimated the effect size (Cohen d) according to Cohen's definition (Cohen, 1992) to detect the statistical power. The levels of small, medium, and large effect size correspond to 0.2, 0.5, and 0.8, respectively. In addition, for the nodal parameter showing significant between-group difference, we further assessed the linear associations between this parameter and the duration of epilepsy in TLE patients by performing Spearman's rank correlation analysis (independent variables: duration of epilepsy; dependent variables: network parameters showing significant between-group differences).

We also compared the differences in S_i^{int} , E_i^{int} , and B_i^{int} for each region (see Supplementary Table S1 for abbreviations of regions) between the epileptogenic and non-epileptogenic hemispheres by using the nonparametric permutation test ($p < 0.05$). Here, for the ITLE patients, we referred to the left hemisphere as the “epileptogenic” hemisphere and the right hemisphere as the “non-epileptogenic” hemisphere. The similar notation was also used for the rTLE patients.

3. Results

3.1. Network parameters

3.1.1. Global parameters

Fig. 1a shows the values of λ and γ changing with sparsity of the whole brain functional networks. We found $\gamma > 1$ and $\lambda \approx 1$ over the range of $0.10 \leq \text{sparsity} \leq 0.24$, which indicates that the networks of all the participants possessed small-world properties (Liao et al., 2010; Zhang et al., 2011).

Fig. 1b shows the other four global parameters (C_w , L_w , E_{loc} , and E_{glob}) changing with the sparsity in the range of $0.10 \leq \text{sparsity} \leq 0.24$ and the statistical between-group comparisons of the global parameters at a given sparsity. For the ITLE patients, we found significantly increased C_w , L_w , and E_{loc} , but significantly decreased E_{glob} compared to the controls at specific sparsity levels (C_w : $0.11 \leq \text{sparsity} \leq 0.24$; L_w and E_{glob} : $0.10 \leq \text{sparsity} \leq 0.14$, 0.18 ; E_{loc} : $0.12 \leq \text{sparsity} \leq 0.14$). For the rTLE patients, no significant changes were detected in any of the global parameters compared to the controls at any sparsity. However, we found that for the rTLE patients, the group-averaged values of C_w , L_w , and E_{loc} were higher, while the group-averaged value of E_{glob} was lower, than those of the controls over the range of $0.10 \leq \text{sparsity} \leq 0.24$.

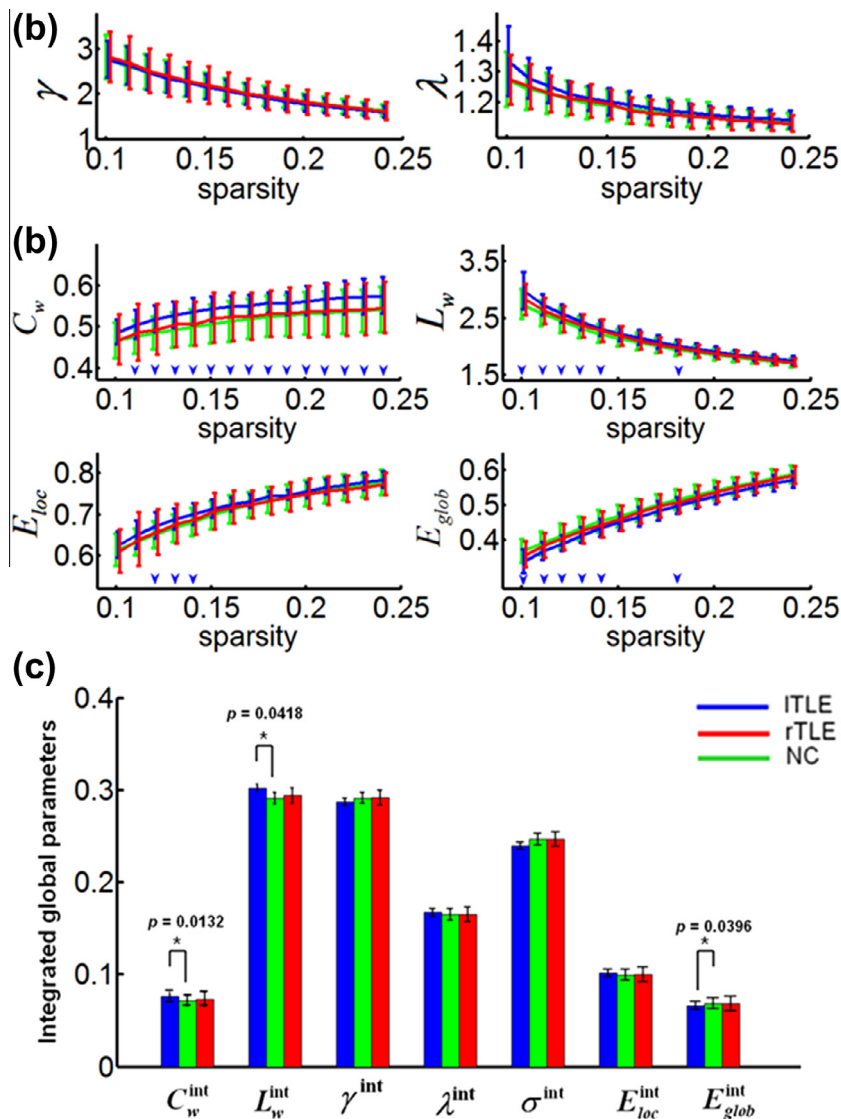


Fig. 1. Global parameters of the whole brain functional networks in left temporal lobe epilepsy (ITLE) patients, right temporal lobe epilepsy (rTLE) patients, and the normal controls (NC). (a) Small-world property. In the range of $0.10 \leq \text{sparsity} \leq 0.24$, the functional networks exhibited $\gamma > 1$ and $\lambda \approx 1$, indicating prominent small-world properties of the brain functional networks for the ITLE patients, rTLE patients, and NC. (b) Global parameters C_w , L_w , E_{loc} , and E_{glob} changing with sparsity. Blue color arrows indicate significant between-group differences at the given sparsity for a given global parameter (permutation test, $p < 0.05$). (c) Bar plots of the integrated global topological parameters of brain functional networks for the ITLE patients, rTLE patients, and controls. The symbol (*) indicates significant between-group differences. Abbreviations: ITLE (rTLE), left (right) temporal lobe epilepsy; C_w , weighted clustering coefficient; L_w , weighted characteristic path length; γ , normalized weighted clustering coefficient; λ , normalized weighted characteristic path length; E_{glob} , global efficiency, E_{loc} , local efficiency. The upscript 'int' stands for the corresponding integrated global parameter. (For interpretation of the references to colour in this figure legend, the reader is referred to the web version of this article.)

Fig. 1c shows the statistical comparisons of the integrated global parameters between either the ITLE or rTLE patients and the controls. For the ITLE patients, we detected a significant increase in the integrated clustering coefficient (C_w^{int}) and integrated characteristic path length (L_w^{int}), but a significant decrease in the integrated global efficiency (E_{glob}^{int}) compared to the controls. For the rTLE patients, no significant between-group difference was detected in any of the integrated global parameters compared to the controls. However, we found that for the rTLE patients, the group-averaged values of C_w^{int} and L_w^{int} were higher, while the group-averaged value of E_{glob}^{int} was lower, than those of the controls.

3.1.2. Nodal parameters

Table 2 lists the brain regions with significant changed integrated nodal strength (S_i^{int}), integrated nodal efficiency (E_i^{int}), and integrated nodal betweenness (B_i^{int}) in either the ITLE or rTLE pa-

tients compared to the controls. Among those integrated nodal parameters, we found only B_i^{int} showed significant alterations in the TLE patients after Bonferroni correction ($p < 0.00056$).

For the ITLE patients, two regions (MTG.R and ORBmid.L) showed significantly increased B_i^{int} , while for the rTLE patients, eight regions (bilateral ANG, HIP.R, IFGtriang.L, ORBsup.R, PCL.R, PHG.L, and IPL.L) showed significantly increased B_i^{int} , compared to the controls. From Table 2, we noticed that the effect size values for these regions reached medium (0.5) or high (0.8) level, suggesting high statistical power for between-group comparisons in nodal parameters. Fig. 2 plots these regions on the cortical surface.

By comparing the between-hemisphere differences in S_i^{int} , E_i^{int} , and B_i^{int} for each region, we found that in ANG and AMYG and other regions listed in Table 3, the nodal parameters in the non-epileptogenic hemisphere were larger than those in the

Table 2

Brain regions showing significant differences in the integrated nodal strength (S_i^{int}), integrated nodal efficiency (E_i^{int}), and integrated nodal betweenness (B_i^{int}) of brain functional networks between either the ITLE or rTLE patients and the normal controls (NC) ($p < 0.05$, Bonferroni correction). Abbreviations: ITLE (rTLE), left (right) temporal lobe epilepsy.

Regions	S_i^{int}		E_i^{int}		B_i^{int}	
	p-Value (Cohen <i>d</i>)	Changes	p-Value (Cohen <i>d</i>)	Changes	p-Value (Cohen <i>d</i>)	Changes
<i>ITLE vs. NC</i>						
MTG.R	0.0162 (0.61)	↑	0.0276 (0.62)	↑	0.0001* (0.56)	↑
ORBmid.L	–	–	–	–	0.0003* (0.53)	↑
<i>rTLE vs. NC</i>						
ANG.L	0.0022 (1.00)	↑	0.0026 (0.91)	↑	0.0001* (0.92)	↑
ANG.R	0.0252 (0.67)	↑	0.0324 (0.64)	↑	0.0001* (1.19)	↑
HIP.R	–	–	–	–	0.0001* (0.43)	↑
IFGtriang.L	–	–	–	–	0.0001* (0.88)	↑
ORBsup.R	–	–	–	–	0.0001* (0.67)	↑
PCL.R	–	–	–	–	0.0001* (0.56)	↑
PHG.L	–	–	–	–	0.0001* (0.45)	↑
IPLL	0.0160 (0.74)	↑	0.0335 (0.63)	↑	0.0001* (0.89)	↑

Note: The symbol ‘↑’ (‘↓’) indicates a significant increase (decrease) in the integrated nodal parameters in the patients group compared to the controls. ‘–’ stands for no significant between-group difference, and ‘*’ for significant difference with Bonferroni correction. Cohen *d* indicates the value of effect size. The levels of small, medium, and large effect size correspond to 0.2, 0.5, and 0.8, respectively.

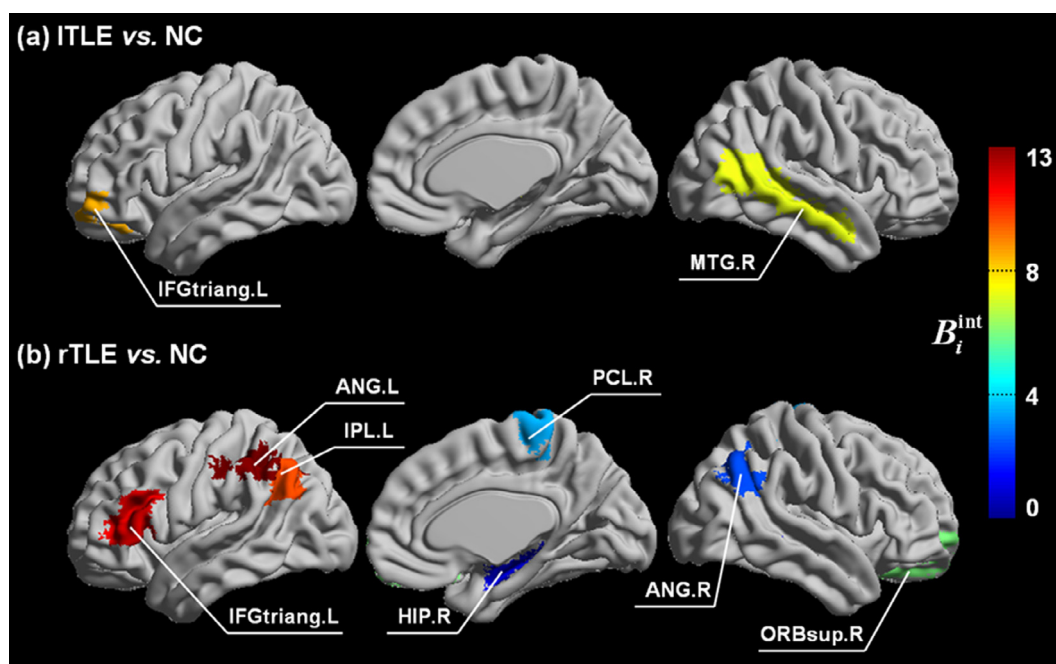


Fig. 2. Surface visualization of brain regions showing significant between-group difference in the integrated nodal betweenness (B_i^{int}) (permutation test, $p < 0.05$, Bonferroni correction). (a) Between ITLE patients and controls; (b) Between rTLE patients and controls. The color bar indicates the value of integrated nodal betweenness (B_i^{int}). Also see Table 3 for more details. ITLE (rTLE), left (right) temporal lobe epilepsy; NC: normal controls. (For interpretation of the references to color in this figure legend, the reader is referred to the web version of this article.)

epileptogenic hemisphere not only for the ITLE patients but also for the rTLE patients ($p < 0.05$) (Table 3).

3.1.3. Hub regions

The hub regions of the brain functional networks for the three participant groups were determined according to Eq. (4) and visually rendered on a model cortex in Fig. 3. We identified eight hubs for the ITLE patients, 12 hubs for the rTLE patients, and 12 hubs for the controls. Among these hubs, two hub regions (MTG.R and SFGdor.) were specific to the ITLE patients, four hub regions (MFG.R, MTG.L, PoCG.L, and PreCG.L) specific to the rTLE patients, and five hub regions (ACG.R, ITG.L, bilateral SMA, and ORBinf.R) specific to the controls. The details of these hubs are listed in Supplementary Table S3.

3.1.4. Robustness of the brain functional network

The results of network robustness analysis under targeted attacks and random failures are shown in Supplementary Fig. S3. We found that both targeted attacks and random failures led to significant network breakdown ($p < 0.05$) across the wide range of removed nodes in both ITLE and rTLE patients. Overall, the networks were more vulnerable to targeted attacks and random failures in the TLE groups relative to the controls.

3.2. Relationships between network parameters and duration of epilepsy

The correlations between either of the altered global or nodal parameters and the duration of epilepsy were analyzed. We

Table 3
Comparisons of integrated nodal parameters, S_i^{int} , E_i^{int} , and B_i^{int} , in each region of the epileptogenic hemisphere (EH) to those in the non-epileptogenic hemisphere (nonEH) for the ITLE and rTLE patients, respectively.

Group	Region	Integrated nodal parameters					
		S_i^{int}		E_i^{int}		S_i^{int}	
		<i>p</i> -value	Change	<i>p</i> -value	Change	<i>p</i> -value	Change
ITLE nonEH (right) vs. EH (left)	ANG	0.0274	↑	0.0356	↑	–	–
	DCG	0.0452	↓	–	–	–	–
	HIP	–	–	–	–	0.0442	↑
	ITG	0.0321	↑	0.0175	↑	–	–
	ORBmid	–	–	–	–	0.0209	↓
	SFGdor	–	–	–	–	0.0397	↑
	SPG	–	–	–	–	0.0485	↓
	THA	–	–	–	–	0.0400	↑
	TPOmid	–	–	–	–	0.0412	↑
rTLE nonEH (left) vs. EH (right)	AMYG	–	–	–	–	0.0353	↑
	IFGtriang	–	–	–	–	0.0323	↑
	MOG	–	–	–	–	0.0269	↑
	MTG	–	–	–	–	0.0434	↑
	PoCG	–	–	–	–	0.0479	↑
	ROL	–	–	–	–	0.0477	↑
	SFGmed	–	–	–	–	0.0264	↑
	SPG	–	–	–	–	0.0082	↑

Note: The symbol of ‘↑’ (‘↓’) indicates a significant increase (decrease) in S_i^{int} , E_i^{int} , and B_i^{int} in non-epileptogenic hemisphere compared to the epileptogenic hemisphere; ‘–’ stands for no significant between-hemisphere difference in the corresponding nodal parameter.

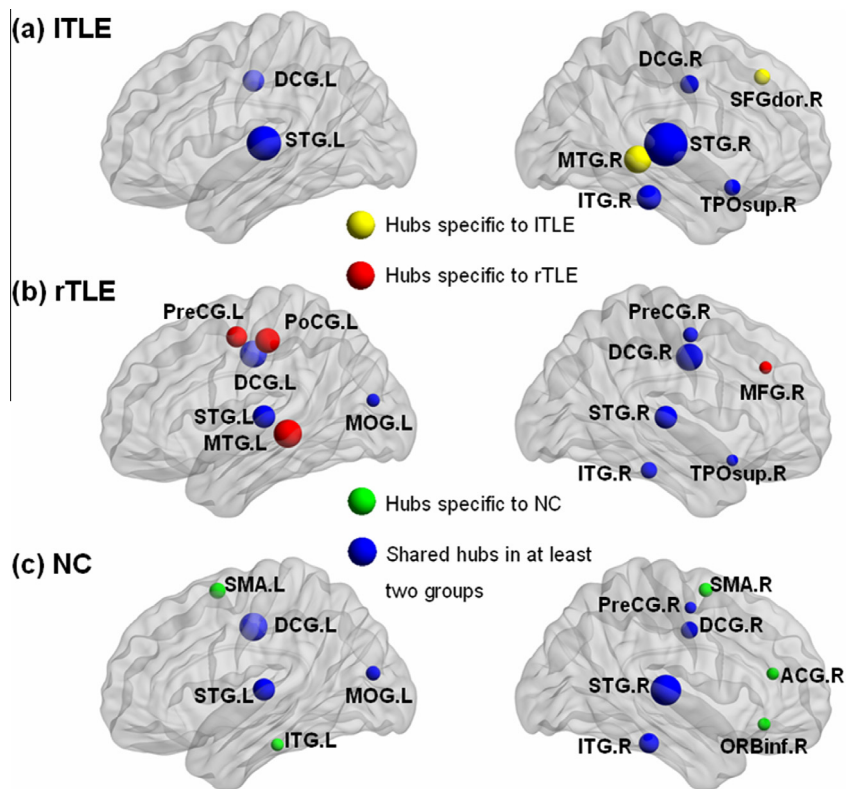


Fig. 3. Surface-rendered plots of hub regions. (a) For ITLE patients, (b) for rTLE patients, and (c) for the controls. The nodal size is proportional to the value of normalized nodal betweenness (B_i^{norm}). ITLE (rTLE), left (right) temporal lobe epilepsy; NC: normal controls.

detected a significantly positive correlation between only E_{loc}^{int} and the duration of epilepsy in the ITLE patients ($p < 0.05$) (Fig. 4). However, for any of the other altered integrated global parameters or nodal parameters, we found no significant correlation with the duration of epilepsy in the ITLE patients. Similarly, we also found none of the altered integrated global parameters or nodal parameters correlated significantly with the duration of epilepsy in the rTLE patients.

3.3. Reproducibility analysis

In order to check our result, we also repeated the calculation with different preprocessing schemes and parcellation schemes, and presented the results in Tables 3 and 4.

For the global parameters, we detected significantly increased integrated clustering coefficient (C_w^{int}) and integrated characteristic path length (L_w^{int}), but significantly decreased integrated global

efficiency (E_{glob}^{int}) in the ITLE patients, no matter which of the preprocessing schemes or which parcellation schemes was selected. On the other hand, in the rTLE patients, we found no significant alteration in any of the global parameters compared to the controls under the main processing scheme. However, when we adopted the schemes of Positive-network, HOA-112, and Dos-160, we detected significantly increased C_w^{int} and L_w^{int} , but significantly decreased B_{glob}^{int} in the rTLE patients, which are consistent with the result detected in the ITLE patients.

For nodal parameters, we detected significantly altered nodal parameters in two regions (MTG.R and ORBmid.L) for the ITLE patients and eight regions (bilateral ANG, HIP.R, IFGtriang.L, ORBsup.R, PCL.R, PHG.L, and IPL.L) for the rTLE patients under the main processing scheme (Fig. 2). When we adopted the other four processing schemes, we found most of these regions (the MTG.R for ITLE patients, as well as the regions of bilateral ANG, HIP.R, IFGtriang.L, ORBsup.R, PCL.R, PHG.L, and IPL.L for the rTLE patients) were always detected in the ITLE or rTLE patients. The consistent results confirmed our results mainly reported in this study.

4. Discussion

In this study, we constructed brain functional networks for all participants, compared the topological properties of the networks between either of the ITLE or rTLE patient groups and the controls, as well as investigated the relationship between the altered topological properties and the duration of epilepsy. The main findings were as follows: (1) significant increase in the clustering

coefficient and characteristic path length but significant decrease in global efficiency were found in the TLE patients compared to the controls; (2) the regions related to altered nodal parameters in the TLE patients are related to the cognitive functions of memory and language; and (3) the local efficiency of the TLE patients was significantly positively correlated with the duration of epilepsy.

4.1. Global parameters

In this study, the brain functional networks for the TLE patient groups and the controls showed a prominent small-world property, a higher clustering coefficient but a lower characteristic path length (Fig. 1a). Small-worldness supports both integrated and distributed information processing and maximizes the efficiency of propagating information at a relatively low cost (Sporns and Honey, 2006).

We also found significantly increased clustering coefficient and characteristic path length, but significantly decreased global efficiency in the TLE patients compared to the controls (Fig. 1 and Table 4) under different processing schemes, which were consistent with several previous studies on brain networks of epilepsy. Vlooswijk et al. (2011) analyzed the brain functional networks of 41 patients with cryptogenic localization-related epilepsy and 23 healthy controls, and detected significantly increased local and decreased global efficiency in epilepsy patients compared to controls. Bernhardt et al. (2011) investigated the structural networks based on cortical thickness correlations in 122 TLE patients and 47 controls, and found the structural networks of TLE patients showed significantly increased path length and clustering compared to controls. In addition, several EEG studies also analyzed network properties of the discharge in epilepsy patients. Ponten et al. (2007) recorded intracerebral EEG signals from seven mesial TLE patients for five periods of interest (interictal, before, during, and after rapid discharge, and postictal), analyzed their network properties, and found that during and after seizures, the brain networks for these patients showed significantly increased clustering coefficient and shortest path length. Bartolomei et al. (2013) recorded the interictal EEG activity in 11 patients with mesial TLE (mTLE group) and eight patients having neocortical epilepsies (non-mTLE group), and found that the clustering coefficient and characteristic path length of the interictal epileptogenic networks were significantly increased in the mTLE group compared to the non-mTLE group.

Although our results were in line with many previous studies, we also found that the alteration directions of the global parameters are not the same to a previous study (Liao et al., 2010). Liao

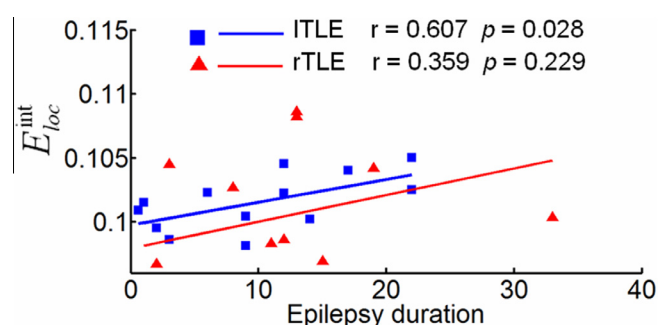


Fig. 4. Scatter plots of the integrated local efficiency (E_{loc}^{int}) changing with the duration of epilepsy in the ITLE and rTLE patients. Significant correlation between E_{loc}^{int} and the duration of epilepsy were detected only in the ITLE patients ($p = 0.028$). ITLE (rTLE), left (right) temporal lobe epilepsy.

Table 4

Reproducibility analysis of alterations in the global parameters of the brain networks between either of the ITLE or rTLE patients and the normal controls (NC) with different preprocessing and parcellation schemes. ITLE (rTLE), left (right) temporal lobe epilepsy.

Reproducibility analysis methods		C_w^{int}	L_w^{int}	E_w^{int}	E_{glob}^{int}	
ITLE vs. NC	Main processing scheme in this study	↑	↑	–	↓	
	Other preprocessing schemes	Smoothing	↑	↑	–	↓
		Positive-network	↑	↑	↑	↓
	Other parcellation schemes	HOA-112	↑	↑	–	↓
		Dos-160	↑	↑	–	↓
rTLE vs. NC	Main processing scheme in this study	–	–	–	–	
	Other preprocessing schemes	Smoothing	–	–	–	–
		Positive-network	↑	–	↑	↓
	Other parcellation schemes	HOA-112	↑	↑	–	↓
		Dos-160	–	↑	–	↓

Note: The ‘↑’ (‘↓’) symbol indicates the global parameter was significantly increased (decreased) in the TLE patients compared to the controls; ‘–’ indicates no significant between-group difference. Smoothing: network analysis based on the correlation matrix constructed from the smoothed rsfMRI data (FWHM = 6 mm); Positive-network, network analysis based on the correlation matrix constructed from the positive-only interregional correlations. AAL-90, the anatomical labeling atlas parcellating the brain into 90 regions; HOA-112, Harvard-Oxford atlas parcellating the brain into 112 regions; Dos-160, Dosenbach atlas consisting of 160 ROIs derived from meta-analysis; C_w^{int} , integrated clustering coefficient; L_w^{int} , integrated characteristic path length; E_{loc}^{int} , integrated local efficiency; E_{glob}^{int} , integrated global efficiency.

et al. (2010) compared the binarized functional networks of TLE patients with controls and revealed significantly decreased clustering coefficient and shortest path length in mTLE patients. This discrepancy may relate to the participants studied or different methodological approaches, binarized or weighted networks. Overall, our results may indicate that the brain functional network in TLE patients tends to be a less optimal network organization, which can also be supported by our robustness analysis results that the TLE patients were more vulnerable to targeted attacks and random failures (Supplementary Fig. S2).

4.2. Nodal parameters

Statistical analysis showed significant differences in the nodal parameters between the TLE patients and the controls. We detected significantly increased values of B_i^{int} in MTG.R for the ITLE patients, and in HIP.R, PHG.L, bilateral ANG, and IPL.L for the rTLE patients under different preprocessing schemes (Tables 2 and 5).

The altered nodal parameters in the regions of HIP.R and PHG.L may indicate the impairment of memory in the TLE patients, which are consistent with several previous studies (Stretton et al., 2012; Voets et al., 2009). Voets et al. (2009) compared the FC between nine ITLE patients and 10 healthy controls, and found significant reductions in FC among different memory-related regions, such as the bilateral mesial temporal lobe, occipital, and left orbitofrontal areas. Stretton et al. (2012) performed a visuospatial “n-back” working memory task to compare the brain activation between 38 TLE patients with unilateral hippocampal sclerosis and 15 healthy controls, and found that the working memory was impaired in unilateral TLE patients and the underlying neural mechanism of working memory was disrupted.

In the rTLE patients, we also found that the value of B_i^{int} was significantly increased in IFGtriang.L (a part of Broca’s area), which

is mainly involved in speech production (Heim et al., 2002; Watkins and Paus, 2004). The impairment of the language system has also been revealed in several previous studies (Brazdil et al., 2005; Jensen et al., 2011). Brazdil et al. (2005) compared the activation pattern during a silent generation task between 13 ITLE patients and 13 controls, and found a significant inter- and intra-hemispheric reorganization of the language-related neuronal networks in ITLE patients. Jensen et al. (2011) mapped the brain activity patterns when TLE patients performed lexical and semantic tasks, and found the obvious increased activation in the left IFG of the language system. Taken together, our findings provide evidence for impairments in cognitive functions of language in TLE patients (Hermann et al., 1992; Mayeux et al., 1980; McDonald et al., 2008).

In addition, we detected that in the rTLE patients, the nodal parameters (integrated nodal strength, S_i^{int} , integrated nodal efficiency, E_i^{int} , and integrated nodal betweenness, B_i^{int}) were significantly increased in the bilateral ANG (Table 2), which are involved in memory retrieval and language (Seghier, 2013). On the other hand, in the ITLE patients, we detected these three nodal parameters were significantly increased in MTG.R, which is involved in several cognitive processes, including memory and language processing (Cabeza and Nyberg, 2000; Chao et al., 1999; Tranel et al., 1997). This finding is consistent with a previous study, in which Zhang et al. (2011) constructed brain functional networks for the idiopathic generalized epilepsy and revealed increased nodal strength and betweenness in MTG.L in TLE patients. Taken together, our findings may provide evidence for disruptions in cognitive functions of memory and language in TLE patients (Hermann et al., 1992; Mayeux et al., 1980; McDonald et al., 2008).

It is worthy to mention that we detected bilateral alterations in the nodal parameters in both ITLE and rTLE patients. Several previous studies (Bettus et al., 2009; Pereira et al., 2010) using

Table 5
 Reproducibility analysis of the brain regions showing significant differences in the integrated nodal strength (S_i^{int}), integrated nodal efficiency (E_i^{int}), and integrated nodal betweenness (B_i^{int}) of the brain functional networks between either the ITLE or rTLE patients and the normal controls (NC) under different preprocessing schemes ($p < 0.05$, Bonferroni correction). ITLE (rTLE), left (right) temporal lobe epilepsy.

Different preprocessing schemes		S_i^{int}	E_i^{int}		B_i^{int}		
		p-Value (Cohen d)	Changes	p-Value (Cohen d)	Changes	p-Value (Cohen d)	Changes
ITLE vs. NC	Smoothing						
	MTG.R	0.0334 (0.65)	↑	–	–	0.0001* (0.76)	↑
	PCG.R	–	–	–	–	0.0001* (0.78)	↑
	Positive-network						
	IPL.L	–	–	–	–	0.0001* (0.47)	↑
	MTG.R	0.0300 (0.65)	↑	0.0328 (0.66)	↑	0.0001* (0.97)	↑
	PAL.R	–	–	–	–	0.0001* (0.72)	↑
rTLE vs. NC	SMG.L	–	–	–	–	0.0003* (0.58)	↑
	Smoothing						
	ANG.L	0.0035 (0.93)	↑	0.0073 (0.84)	↑	0.0001* (1.05)	↑
	ANG.R	0.0304 (0.65)	↑	0.0415 (0.61)	↑	0.0001* (1.29)	↑
	IFGtriang.L	–	–	–	–	0.0001* (0.98)	↑
	IPL.L	0.0321 (0.64)	↑	–	–	0.0001* (0.58)	↑
	IPL.R	–	–	–	–	0.0001* (1.01)	↑
	MTG.L	0.0339 (0.62)	↑	0.0218 (0.71)	↑	0.0001* (1.02)	↑
	MTG.R	–	–	–	–	0.0001* (0.78)	↑
	PCL.R	–	–	–	–	0.0001* (0.47)	↑
	Positive-network						
	IPL.L	0.0165 (0.73)	↑	0.0276 (0.65)	↑	0.0001* (0.79)	↑
	IPL.R	0.0248 (0.68)	↑	–	–	0.0001* (0.75)	↑
	ORBsup.R	–	–	–	–	0.0001* (0.72)	↑
	PCL.R	–	–	–	–	0.0001* (0.63)	↑
PHG.L	–	–	–	–	0.0001* (0.51)	↑	

Note: The symbol ‘↑’ (‘↓’) indicates a significant increase (decrease) in S_i^{int} , E_i^{int} , or B_i^{int} ; ‘–’ stands for no significant between-group difference, and ‘*’ for significant with Bonferroni correction. Smoothing: network analysis based on the correlation matrix constructed from the smoothed rsfMRI data (FWHM = 6 mm); Positive-network, network analysis based on the correlation matrix constructed from the positive-only interregional correlations. The text shaded in gray represents the detected regions showing significant between-group difference under the main preprocessing scheme in this study. Cohen d indicates the value of effect size. The small, medium, and large levels of the effect size are 0.2, 0.5, and 0.8, respectively.

ROI-wise analysis found unilateral TLE patients are associated with functional alterations in bilateral hemispheres, while others using ICA (Voets et al., 2012; Zhang et al., 2010) detected functional alterations in the ipsilateral hemisphere. Whether functional alterations can be detected in the bilateral or ipsilateral hemisphere in unilateral TLE patients may reflect the sensitivity of processing methods applied in the rsfMRI studies, such as ROI-wise analysis (Bettus et al., 2009; Pereira et al., 2010) or ICA (Voets et al., 2012; Zhang et al., 2010). For example, Bettus et al. (2009) selected five ROIs (BA 38; AMY, amygdale; EC, entorhinal cortex; AntHip, anterior hippocampus; and PostHip, posterior hippocampus) in TLE epileptogenic networks, calculated interregional FC, and revealed that the FC of the link AntHip.L-PostHip.L in the left hemisphere was significantly decreased, but FC of the link AntHip.R-PostHip.R in the right hemisphere was significantly increased in ITLE patients. On the other hand, Voets et al. (2012) used ICA to process rsfMRI data in 35 TLE patients and 20 controls, and found significantly decreased FCs which were located in the ipsilateral temporal cortex in ITLE patients.

In this study, we also detected the differences in nodal parameters between the epileptogenic and the non-epileptogenic hemispheres in the ITLE and rTLE patients, respectively (Table 3), which were consistent with several previous studies (Akanuma et al., 2003, 2009; Ferrier et al., 2000). Ferrier et al. (2000) performed proton MRS and the intracarotid amobarbital test (IAT) in 16 TLE patients and calculated the metabolite ratios. They found that the total memory score, memory for objects and faces, and the ratio between N-acetylaspartate (NAA) and creatine and phosphocreatine (Cr + PCr) were significantly lower for the ipsilateral hemisphere than those in the contralateral hemisphere. Akanuma et al. (2009) performed a PET study to measure the interictal cerebral metabolism, and found the memory scores in the right hemisphere was correlated with the metabolite ratios in the right frontotemporal regions, whereas the memory scores in the left hemisphere was correlated with the metabolite ratios in left lateral and medial temporal regions. However, Lacruz et al. (2007) recorded the intracranial EEG response in several regions, such as the medial temporal and entorhinal cortices, to electrical stimulation in 51 epilepsy patients, and revealed no difference in intracranial EEG response between epileptogenic and non-epileptogenic hemispheres. Whether the differences between epileptogenic and non-epileptogenic hemispheres existed in unilateral TLE patients may reflect the sensitivity of the research method. It may be that the electrical stimulus is relatively less sensitive than other methods. Further, the finding that the integrated nodal parameters in the non-epileptogenic hemisphere were larger than those in the epileptogenic hemisphere may reflect the effects of the focal side on impairments in brain functional networks of TLE patients (Ahmadi et al., 2009; Ferrier et al., 2000; Pail et al., 2010).

4.3. Clinical relevance of network alterations

In this study, we found a positive correlation between the altered the integrated local efficiency (E_{loc}^{int}) and the epilepsy duration in TLE patients (Fig. 4). The increased E_{loc}^{int} indicates that the networks of TLE patients tend to be regular ones. Shifts of the networks toward either random (Liu et al., 2008; Supekar et al., 2008) or regular networks (De Vico Fallani et al., 2007; Wang et al., 2009b) reflect that the networks for TLE patients are less optimal. The positive correlation between E_{loc}^{int} and epilepsy duration may suggest that as the disease develops, the whole brain functional networks in TLE patients tend to show more regular network organization. These results may reflect the progress of TLE pathology over time or disease severity.

The significant correlation between E_{loc}^{int} and epilepsy duration is in agreement with several previous studies (Bartolomei et al.,

2013; van Dellen et al., 2009) that suggested network property changes over time in TLE patients. Bartolomei et al. (2013) recorded intracerebral EEG signals from patients with drug-resistant epilepsies during the interictal period, analyzed the basal properties of epileptogenic networks, and found that the small-worldness was negatively correlated with the epilepsy duration. Similarly, Van Dellen et al. (2009) recorded the interictal electrocorticography (ECoG) signals from 27 TLE patients at the time of surgery, assessed the FC of the temporal lobe by using the phase lag index, and revealed that the average FC, clustering coefficient, and small-worldness were negatively correlated with the epilepsy duration.

In addition, the increased E_{loc}^{int} with the increased epilepsy duration in ITLE patients may result from the brain functional compensatory mechanism, which has been suggested in previous studies in TLE patients (Addis et al., 2007; Bettus et al., 2009; Holmes et al., 2014; Maguire et al., 2001; Powell et al., 2007; Thivard et al., 2005). The local efficiency of a brain network, which is predominantly associated with short-range FCs (He et al., 2009), measures the performance of information exchanging in a sub-network (Rubinov and Sporns, 2010); that is, when the global efficiency is decreased in TLE patients, the short-range path length for information exchange tends to increase to sustain the whole brain functions as a compensatory mechanism. This also indicates the importance of brains' segregated neural processing as diseases developed (Rubinov and Sporns, 2010). In addition, we also found increased local efficiency (E_i^{int}) in MTG.R in ITLE patients (Table 2).

However, we only found a significant correlation between E_{loc}^{int} and epilepsy duration ($r = 0.607$, $p = 0.028$). Similarly, a few studies (Bartolomei et al., 2013; van Dellen et al., 2009) have tried to determine the significant correlation between network parameters and epilepsy duration. For example, Bartolomei et al. (2013) applied graph analysis to intracerebral EEG recordings of 11 mTLE patients during the interictal period, and found no correlations between several other parameters, such as the clustering coefficient and characteristic path length, and the epilepsy duration, though they revealed a significantly positive correlation between the small-world index S and the epilepsy duration ($p = 0.020$). Strong or weak correlation between a selective parameter and the epilepsy duration may reflect the different sensitivity to specific clinical variables. In addition, only in the ITLE patients, but not in the rTLE patients, we found significant correlation between E_{loc}^{int} and epilepsy duration, which may suggest the differences in network parameter alterations between ITLE and rTLE patients. Distinguishing the differences between ITLE and rTLE patients is an interesting topic and these differences have been investigated in many previous studies (Ahmadi et al., 2009; Bettus et al., 2009; Haneef et al., 2012; Pail et al., 2010).

4.4. Comparisons between ITLE and rTLE

In this study, we observed different alterations in nodal parameters between ITLE and rTLE patients, which were consistent with previous studies (Ahmadi et al., 2009; Bettus et al., 2009; Haneef et al., 2012; Pail et al., 2010). Bettus et al. (2009) compared the FC between either of the ITLE or rTLE patients and the controls, and found FC between the left entorhinal cortex and left anterior hippocampus was significantly decreased in ITLE, but significantly increased in rTLE. Pail et al. (2010) analyzed brain structural changes in TLE patients, and revealed that the brain morphological changes were more pronounced in rTLE patients than in ITLE patients. Ahmadi et al. (2009) analyzed diffusion MRI data and found that the reduction of fiber anisotropy exists in both ipsilateral and contralateral hemispheres for ITLE patients, but only in the ipsilateral hemisphere for rTLE patients. Haneef et al. (2012) acquired rsfMRI data from 11 rTLE, 12 ITLE, and 13 controls, analyzed the

FC of two ROIs (ventromedial prefrontal cortex: vmPFC; retrosplenium/precuneus: PCUN/Rsp) in the DMN, and detected the differences between ITLE and rTLE with increased FC between the PCUN/Rsp and opercular as well as increased FC between vmPFC and fronto-centro-parietal in ITLE, but decreased FC between PCUN/Rsp and right anteromedial temporal in rTLE, compared to controls.

We also compared the difference in network parameters between ITLE and rTLE patients, and the results are presented in [Supplementary Figs. S3 and S4](#).

4.5. Limitations

Several limit factors need to be addressed. First, we did not consider the negative influences of the antiepileptic drug on FC ([Waites et al., 2006](#)), despite the fact that the patients had discontinued medication for about 24 h in the present study. In addition, the potential effects of interictal epileptiform discharges on the brain functional network were not evaluated because we lacked simultaneous EEG-fMRI data of TLE patients. Second, we unfortunately did not perform the neuropsychological tests, such as the Intracarotid Amobarbital Test and Wechsler Memory Scale Test ([Doucet et al., 2013](#); [Ferrier et al., 2000](#)), though they may be used to associate with the network parameters. Neuropsychological tests can be used to test various cognitive functions in TLE patients. In addition, cognitive impairment, particularly memory and language disruption, is a major complicating feature of epilepsy ([Bell et al., 2011](#); [Lambon Ralph et al., 2010, 2012](#)). In the future study, we need to conduct some important neuropsychological tests to see if there exists a significant correlation between the network parameters and the neuropsychological test scores. Third, the low signal to noise ratio (SNR) of the rsfMRI data acquired from a 1.5 T MRI scanner may be not optimized for performing a BOLD-based network analysis ([Triantafyllou et al., 2005](#)). We noticed that the temporal resolution or sampling rate $TR = 3$ s of the rsfMRI data was low in this study. Under this sampling rate, respiratory and cardiac fluctuations, which would reduce the specificity of low-frequency fluctuations to functional connected regions ([Lowe et al., 1998](#)), may be unavoidable in fMRI time series, even though a band-pass filtering of 0.01–0.08 Hz was used to reduce physiological noise. In addition, the spatial resolution (voxel = $1.8 \times 1.8 \times 4.5$ mm) was not high. Under this spatial resolution, the BOLD signal was affected by the coupling between BOLD and underlying vasculature signals ([Ugurbil et al., 2003](#)).

5. Conclusion

In summary, we explored the topological alterations in the whole brain functional networks of TLE patients using graph theory analysis and investigated the relationship between the altered topological properties and the duration of epilepsy. We detected a significant increase in clustering coefficient and characteristic path length, but a significant decrease in global efficiency in TLE patients, compared to the controls, which may indicate a loss of optimal topological organization of brain functional networks in TLE patients. We also found that the regions showing altered nodal parameters in the TLE patients are located in the DMN, and are related to cognitive functions of memory and language, which may reflect TLE-related impairment of the DMN, memory, and language systems. This study also revealed that the local efficiency of the TLE patients was significantly positively correlated with the epilepsy duration. In summary, these findings can help us understand the clinical symptoms of TLE patients, such as abnormal behaviors, worse memory, and poor language performance. In addition, these detected impairments of the whole brain functional networks may

have offered a clue for the diagnosis and treatment of the TLE patients in the future. Generally speaking, clarifying the origin of the functional abnormalities and detecting their progression over time in epilepsy present a challenge to neurologists. Although the network analysis may not provide a direct tool to diagnose TLE patients from a clinical point, it indeed provides extra information on the disrupted whole brain functional networks in TLE patients ([Craddock et al., 2013](#)). Thus, all efforts should be made, therefore, to control seizures through drug treatments or surgical intervention ([Seeck, 2013](#)).

Acknowledgments

This work was partly supported by the Guangdong 999 Brain Hospital, the funding of the National Natural Science Foundation of China, China (Grant numbers: 81071149, 81271548, 81271389, and 81371535), the Science and Technology Planning Project of Guangdong Province (2011b060200002), and the Scientific Research Foundation for Returned Overseas Chinese Scholars (R.H.), State Education Ministry. The authors express their appreciation to Drs. Rhoda E. and Edmund F. Perozzi for editing assistance. The authors declare that they have no competing financial interests.

Appendix A. Supplementary data

Supplementary data associated with this article can be found, in the online version, at <http://dx.doi.org/10.1016/j.clinph.2013.12.120>.

References

- Achard S, Bullmore E. Efficiency and cost of economical brain functional networks. *PLoS Comput Biol* 2007;3:e17.
- Addis DR, Moscovitch M, McAndrews MP. Consequences of hippocampal damage across the autobiographical memory network in left temporal lobe epilepsy. *Brain* 2007;130:2327–42.
- Ahmadi ME, Hagler Jr DJ, McDonald CR, Tecoma ES, Iragui VJ, Dale AM, et al. Side matters: diffusion tensor imaging tractography in left and right temporal lobe epilepsy. *AJNR Am J Neuroradiol* 2009;30:1740–7.
- Akanuma N, Alarcon G, Lum F, Kissani N, Koutroumanidis M, Adachi N, et al. Lateralising value of neuropsychological protocols for presurgical assessment of temporal lobe epilepsy. *Epilepsia* 2003;44:408–18.
- Akanuma N, Reed LJ, Marsden PK, Jarosz J, Adachi N, Hallett WA, et al. Hemisphere-specific episodic memory networks in the human brain: a correlation study between intracarotid amobarbital test and [(18)F]FDG-PET. *J Cogn Neurosci* 2009;21:605–22.
- Akman CI, Ichise M, Olsavsky A, Tikofsky RS, Van Heertum RL, Gilliam F. Epilepsy duration impacts on brain glucose metabolism in temporal lobe epilepsy: results of voxel-based mapping. *Epilepsy Behav* 2010;17:373–80.
- Anand A, Li Y, Wang Y, Lowe MJ, Dzemidzic M. Resting state corticolimbic connectivity abnormalities in unmedicated bipolar disorder and unipolar depression. *Psychiatry Res* 2009;171:189–98.
- Bartolomei F, Bettus G, Stam CJ, Guye M. Interictal network properties in mesial temporal lobe epilepsy: a graph-theoretical study from intracerebral recordings. *Clin Neurophysiol* 2013;124:2345–53.
- Bassett DS, Bullmore E. Small-world brain networks. *Neuroscientist* 2006;12:512–23.
- Bell B, Lin JJ, Seidenberg M, Hermann B. The neurobiology of cognitive disorders in temporal lobe epilepsy. *Nat Rev Neurol* 2011;7:154–64.
- Bernhardt BC, Rozen DA, Worsley KJ, Evans AC, Bernasconi N, Bernasconi A. Thalamo-cortical network pathology in idiopathic generalized epilepsy: insights from MRI-based morphometric correlation analysis. *NeuroImage* 2009;46:373–81.
- Bernhardt BC, Chen Z, He Y, Evans AC, Bernasconi N. Graph-theoretical analysis reveals disrupted small-world organization of cortical thickness correlation networks in temporal lobe epilepsy. *Cereb Cortex* 2011;21:2147–57.
- Bernhardt BC, Bernasconi N, Kim H, Bernasconi A. Mapping thalamocortical network pathology in temporal lobe epilepsy. *Neurology* 2012;78:129–36.
- Bettus G, Guedj E, Joyeux F, Confort-Gouny S, Soulier E, Laguitton V, et al. Decreased basal fMRI functional connectivity in epileptogenic networks and contralateral compensatory mechanisms. *Hum Brain Mapp* 2009;30:1580–91.
- Bonilha L, Rorden C, Castellano G, Pereira F, Rio PA, Cendes F, et al. Voxel-based morphometry reveals gray matter network atrophy in refractory medial temporal lobe epilepsy. *Arch Neurol – Chicago* 2004;61:1379–84.

- Braun U, Plichta MM, Esslinger C, Sauer C, Haddad L, Grimm O, et al. Test-retest reliability of resting-state connectivity network characteristics using fMRI and graph theoretical measures. *NeuroImage* 2012;59:1404–12.
- Brazdil M, Chlebus P, Mikl M, Pazourkova M, Krupa P, Rektor I. Reorganization of language-related neuronal networks in patients with left temporal lobe epilepsy – an fMRI study. *Eur J Neurol* 2005;12:268–75.
- Bullmore E, Sporns O. Complex brain networks: graph theoretical analysis of structural and functional systems. *Nat Rev Neurosci* 2009;10:186–98.
- Bullmore ET, Suckling J, Overmeyer S, Rabe-Hesketh S, Taylor E, Brammer MJ. Global, voxel, and cluster tests, by theory and permutation, for a difference between two groups of structural MR images of the brain. *IEEE Trans Med Imaging* 1999;18:32–42.
- Cabeza R, Nyberg L. Imaging cognition II: an empirical review of 275 PET and fMRI studies. *J Cogn Neurosci* 2000;12:1–47.
- Chao LL, Haxby JV, Martin A. Attribute-based neural substrates in temporal cortex for perceiving and knowing about objects. *Nat Neurosci* 1999;2:913–9.
- Cohen J. A power primer. *Psychol Bull* 1992;112:155–9.
- Craddock RC, Jbabdi S, Yan C-G, Vogelstein JT, Castellanos FX, Di Martino A, et al. Imaging human connectomes at the macroscale. *Nat Methods* 2013;10:524–39.
- de Reus MA, van den Heuvel MP. The parcellation-based connectome: limitations and extensions. *NeuroImage* 2013;80:397–404.
- de Vico Fallani F, Astolfi L, Cincotti F, Mattia D, Marciani MG, Salinari S, et al. Cortical functional connectivity networks in normal and spinal cord injured patients: evaluation by graph analysis. *Hum Brain Mapp* 2007;28:1334–46.
- Dosenbach NUF, Nardos B, Cohen AL, Fair DA, Power JD, Church JA, et al. Prediction of individual brain maturity using fMRI. *Science* 2010;329:1358–61.
- Doucet G, Osipowicz K, Sharan A, Sperling MR, Tracy JL. Extratemporal functional connectivity impairments at rest are related to memory performance in mesial temporal epilepsy. *Hum Brain Mapp* 2013;34:2202–16.
- Edefonti V, Bravi F, Turner K, Beghi E, Canevini MP, Ferraroni M, et al. Health-related quality of life in adults with epilepsy: the effect of age, age at onset and duration of epilepsy in a multicentre Italian study. *BMC Neurol* 2011;11:33.
- Ferrier CH, Alarcon G, Glover A, Koutroumanidis M, Morris RG, Simmons A, et al. N-acetylaspartate and creatine levels measured by (1)H MRS relate to recognition memory. *Neurology* 2000;55:1874–83.
- Fornito A, Zalesky A, Bullmore ET. Network scaling effects in graph analytic studies of human resting-state fMRI data. *Front Syst Neurosci* 2010;4:22.
- Fox MD, Snyder AZ, Vincent JL, Corbetta M, Van Essen DC, Raichle ME. The human brain is intrinsically organized into dynamic, anticorrelated functional networks. *PNAS* 2005;102:9673–8.
- Fox MD, Zhang D, Snyder AZ, Raichle ME. The global signal and observed anticorrelated resting state brain networks. *J Neurophysiol* 2009;101:3270–83.
- Greicius M. Resting-state functional connectivity in neuropsychiatric disorders. *Curr Opin Neurol* 2008;21:424–30.
- Gupta VK, Singh AK, Gupta B. Development of membrane electrodes for selective determination of some antiepileptic drugs in pharmaceuticals, plasma and urine. *Anal Bioanal Chem* 2007;389:2019–28.
- Guye M, Regis J, Tamura M, Wendling F, McGonigal A, Chauvel P, et al. The role of corticothalamic coupling in human temporal lobe epilepsy. *Brain* 2006;129:1917–28.
- Haneef Z, Lenartowicz A, Yeh HJ, Engel Jr J, Stern JM. Effect of lateralized temporal lobe epilepsy on the default mode network. *Epilepsy Behav* 2012;25:350–7.
- He Y, Evans A. Graph theoretical modeling of brain connectivity. *Curr Opin Neurol* 2010;23:341–50.
- He Y, Chen Z, Evans A. Structural insights into aberrant topological patterns of large-scale cortical networks in Alzheimer's disease. *J Neurosci* 2008;28:4756–66.
- He Y, Dagher A, Chen Z, Charil A, Zijdenbos A, Worsley K, et al. Impaired small-world efficiency in structural cortical networks in multiple sclerosis associated with white matter lesion load. *Brain* 2009;132:3366–79.
- Heim S, Opitz B, Friederici AD. Broca's area in the human brain is involved in the selection of grammatical gender for language production: evidence from event-related functional magnetic resonance imaging. *Neurosci Lett* 2002;328:101–4.
- Hermann BP, Seidenberg M, Haltiner A, Wyler AR. Adequacy of language function and verbal memory performance in unilateral temporal lobe epilepsy. *Cortex* 1992;28:423–33.
- Holmes M, Folley BS, Sonmezurk HH, Gore JC, Kang H, Abou-Khalil B, et al. Resting state functional connectivity of the hippocampus associated with neurocognitive function in left temporal lobe epilepsy. *Hum Brain Mapp* 2014;35:735–44.
- Humphries MD, Gurney K, Prescott TJ. The brainstem reticular formation is a small-world, not scale-free, network. *Proc Biol Sci* 2006;273:503–11.
- ILAE. Proposal for revised classification of epilepsies and epileptic syndromes. commission on classification and terminology of the international league against epilepsy. *Epilepsia* 1989;30:389–99.
- Jensen EJ, Hargreaves I, Bass A, Pexman P, Goodyear BG, Federico P. Cortical reorganization and reduced efficiency of visual word recognition in right temporal lobe epilepsy: a functional MRI study. *Epilepsy Res* 2011;93:155–63.
- Kennedy DN, Lange N, Makris N, Bates J, Meyer J, Caviness Jr VS. Gyri of the human neocortex: an MRI-based analysis of volume and variance. *Cereb Cortex* 1998;8:372–84.
- Lacruz ME, Garcia Seoane JJ, Valentin A, Selway R, Alarcon G. Frontal and temporal functional connections of the living human brain. *Eur J Neurol* 2007;26:1357–70.
- Lambon Ralph MA, Cipolletti L, Manes F, Patterson K. Taking both sides: do unilateral anterior temporal lobe lesions disrupt semantic memory? *Brain* 2010;133:3243–55.
- Lambon Ralph MA, Ehsan S, Baker GA, Rogers TT. Semantic memory is impaired in patients with unilateral anterior temporal lobe resection for temporal lobe epilepsy. *Brain* 2012;135:242–58.
- Liao W, Zhang Z, Pan Z, Mantini D, Ding J, Duan X, et al. Altered functional connectivity and small-world in mesial temporal lobe epilepsy. *Plos One* 2010;5:e8525.
- Liao W, Zhang Z, Pan Z, Mantini D, Ding J, Duan X, et al. Default mode network abnormalities in mesial temporal lobe epilepsy: a study combining fMRI and DTI. *Hum Brain Mapp* 2011;32:883–95.
- Liu Y, Liang M, Zhou Y, He Y, Hao Y, Song M, et al. Disrupted small-world networks in schizophrenia. *Brain* 2008;131:945–61.
- Lowe MJ, Mock BJ, Sorenson JA. Functional connectivity in single and multislice echoplanar imaging using resting-state fluctuations. *NeuroImage* 1998;7:119–32.
- Lynall ME, Bassett DS, Kerwin R, McKenna PJ, Kitzbichler M, Muller U, et al. Functional connectivity and brain networks in schizophrenia. *J Neurosci* 2010;30:9477–87.
- Maguire EA, Vargha-Khadem F, Mishkin M. The effects of bilateral hippocampal damage on fMRI regional activations and interactions during memory retrieval. *Brain* 2001;124:1156–70.
- Mayeux R, Brandt J, Rosen J, Benson DF. Interictal memory and language impairment in temporal lobe epilepsy. *Neurology* 1980;30:120–5.
- McDonald CR, Ahmadi ME, Hagler DJ, Tecoma ES, Iragui VJ, Gharapetian L, et al. Diffusion tensor imaging correlates of memory and language impairments in temporal lobe epilepsy. *Neurology* 2008;71:1869–76.
- Morgan VL, Gore JC, Abou-Khalil B. Functional epileptic network in left mesial temporal lobe epilepsy detected using resting fMRI. *Epilepsy Res* 2010;88:168–78.
- Pail M, Brazdil M, Marecek R, Mikl M. An optimized voxel-based morphometric study of gray matter changes in patients with left-sided and right-sided mesial temporal lobe epilepsy and hippocampal sclerosis (MTLE/HS). *Epilepsia* 2010;51:511–8.
- Pereira FR, Alessio A, Sercheli MS, Pedro T, Bilevicius E, Rondina JM, et al. Asymmetrical hippocampal connectivity in mesial temporal lobe epilepsy: evidence from resting state fMRI. *BMC Neurosci* 2010;11:66.
- Ponten SC, Bartolomei F, Stam CJ. Small-world networks and epilepsy: graph theoretical analysis of intracerebrally recorded mesial temporal lobe seizures. *Clin Neurophysiol* 2007;118:918–27.
- Powell HWR, Richardson MP, Symms MR, Boulby PA, Thompson PJ, Duncan JS, et al. Reorganization of verbal and nonverbal memory in temporal lobe epilepsy due to unilateral hippocampal sclerosis. *Epilepsia* 2007;48:1512–25.
- Rubinov M, Sporns O. Complex network measures of brain connectivity: uses and interpretations. *NeuroImage* 2010;52:1059–69.
- Seeck M. Epilepsy: repeat MRI in patients with chronic epilepsy. *Nat Rev Neurol* 2013;9:545–6.
- Seghier ML. The angular gyrus: multiple functions and multiple subdivisions. *Neuroscientist* 2013;19:43–61.
- Sidhu MK, Stretton J, Winston GP, Bonelli S, Centeno M, Vollmar C, et al. A functional magnetic resonance imaging study mapping the episodic memory encoding network in temporal lobe epilepsy. *Brain* 2013;136:1868–88.
- Sporns O, Honey CJ. Small worlds inside big brains. *Proc Natl Acad Sci USA* 2006;103:19219–20.
- Stretton J, Winston G, Sidhu M, Centeno M, Vollmar C, Bonelli S, et al. Neural correlates of working memory in temporal lobe epilepsy – an fMRI study. *NeuroImage* 2012;60:1696–703.
- Supekar K, Menon V, Rubin D, Musen M, Greicius MD. Network analysis of intrinsic functional brain connectivity in Alzheimer's disease. *PLoS Comput Biol* 2008;4:e1000100.
- Thivard L, Hombrock J, du Montcel ST, Delmaire C, Cohen L, Samson S, et al. Productive and perceptive language reorganization in temporal lobe epilepsy. *NeuroImage* 2005;24:841–51.
- Tian L, Wang J, Yan C, He Y. Hemisphere- and gender-related differences in small-world brain networks: a resting-state functional MRI study. *NeuroImage* 2011;54:191–202.
- Tranel D, Damasio H, Damasio AR. A neural basis for the retrieval of conceptual knowledge. *Neuropsychologia* 1997;35:1319–27.
- Triantafyllou C, Hoge RD, Krueger G, Wiggins CJ, Potthast A, Wiggins GC, et al. Comparison of physiological noise at 1.5 T, 3 T and 7 T and optimization of fMRI acquisition parameters. *NeuroImage* 2005;26:243–50.
- Tzourio-Mazoyer N, Landeau B, Papathanassiou D, Crivello F, Etard O, Delcroix N, et al. Automated anatomical labeling of activations in SPM using a macroscopic anatomical parcellation of the MNI MRI single-subject brain. *NeuroImage* 2002;15:273–89.
- Ugurbil K, Toth L, Kim DS. How accurate is magnetic resonance imaging of brain function? *Trends Neurosci* 2003;26:108–14.
- van Dellen E, Douw L, Baayen JC, Heimans JJ, Ponten SC, Vandertop WP, et al. Long-term effects of temporal lobe epilepsy on local neural networks: a graph theoretical analysis of corticography recordings. *Plos One* 2009;4.
- van den Heuvel MP, Hulshoff Pol HE. Exploring the brain network: a review on resting-state fMRI functional connectivity. *Eur Neuropsychopharmacol* 2010;20:519–34.
- Vlooswijk MC, Vaessen MJ, Jansen JF, de Krom MC, Majoie HJ, Hofman PA, et al. Loss of network efficiency associated with cognitive decline in chronic epilepsy. *Neurology* 2011;77:938–44.
- Voets NL, Adcock JE, Stacey R, Hart Y, Carpenter K, Matthews PM, et al. Functional and structural changes in the memory network associated with left temporal lobe epilepsy. *Hum Brain Mapp* 2009;30:4070–81.

- Voets NL, Beckmann CF, Cole DM, Hong S, Bernasconi A, Bernasconi N. Structural substrates for resting network disruption in temporal lobe epilepsy. *Brain* 2012;135:2350–7.
- Waites AB, Briellmann RS, Saling MM, Abbott DF, Jackson GD. Functional connectivity networks are disrupted in left temporal lobe epilepsy. *Ann Neurol* 2006;59:335–43.
- Wang J, Wang L, Zang Y, Yang H, Tang H, Gong Q, et al. Parcellation-dependent small-world brain functional networks: a resting-state fMRI study. *Hum Brain Mapp* 2009a;30:1511–23.
- Wang L, Zhu C, He Y, Zang Y, Cao Q, Zhang H, et al. Altered small-world brain functional networks in children with attention-deficit/hyperactivity disorder. *Hum Brain Mapp* 2009b;30:638–49.
- Wang JH, Zuo XN, Gohel S, Milham MP, Biswal BB, He Y. Graph theoretical analysis of functional brain networks: test-retest evaluation on short- and long-term resting-state functional MRI data. *Plos One* 2011;6:e21976.
- Watkins K, Paus T. Modulation of motor excitability during speech perception: the role of Broca's area. *J Cogn Neurosci* 2004;16:978–87.
- Watts DJ, Strogatz SH. Collective dynamics of 'small-world' networks. *Nature* 1998;393:440–2.
- Yan C, Zang Y. DPARSF: A MATLAB toolbox for "Pipeline" data analysis of resting-state fMRI. *Front Syst Neurosci* 2010;4:13.
- Zhang Z, Lu G, Zhong Y, Tan Q, Liao W, Chen Z, et al. Impaired perceptual networks in temporal lobe epilepsy revealed by resting fMRI. *J Neurol* 2009a;256:1705–13.
- Zhang Z, Lu G, Zhong Y, Tan Q, Yang Z, Liao W, et al. Impaired attention network in temporal lobe epilepsy: a resting FMRI study. *Neurosci Lett* 2009b;458:97–101.
- Zhang Z, Lu G, Zhong Y, Tan Q, Liao W, Wang Z, et al. Altered spontaneous neuronal activity of the default-mode network in mesial temporal lobe epilepsy. *Brain Res* 2010;1323:152–60.
- Zhang Z, Liao W, Chen H, Mantini D, Ding JR, Xu Q, et al. Altered functional-structural coupling of large-scale brain networks in idiopathic generalized epilepsy. *Brain* 2011;134:2912–28.
- Zheng JN, Qin BL, Dang C, Ye W, Chen ZR, Yu L. Alertness network in patients with temporal lobe epilepsy: a fMRI study. *Epilepsy Res* 2012;100:67–73.